

Quench simulations of a superconducting composite model in a modified CLIQ system using split coils and simultaneous overcurrent

X. Zhang¹, L. Lu², E.W. Collings¹, and M.D. Sumption¹

¹CSMM, MSE, The Ohio State University, Columbus, OH 43210, USA

²Department of Radiation Oncology, The Ohio State University Wexner Medical Center, Columbus, OH 43210, USA

Email: zhang.10444@osu.edu

Abstract. The numerical simulation of a quench protection system applicable to a MgB₂-wound 3T conduction cooled magnetic resonance imaging (MRI) magnet is described. This study uses a lumped parameter model in Open Modelica. Modelica is an equation-based, object-oriented language that excels in modelling physical systems. Our initial approach was similar to a coupling-loss induced quench (CLIQ) model, which we applied to a coil of MgB₂ strand. In previous simulations, the capacitor, and other component sizes and ratings were determined. However, the large maximum voltage was required for this CLIQ system to prevent risking a voltage breakdown and coil damage. In a modified CLIQ system, we split the coil in such a way to reduce the inductance and resultant maximum voltage of the pair. A lumped parameter model built in Open Modelica described the resistance of the coil for operating currents larger than critical current ($I > I_c$). We went on to achieve protective heating by (a) directly driving the coil into overcurrent for and (b) inducing AC loss. This mixed approach uses split coils and a Joule heated matrix. Testing was modelling with various capacitor sizes and charged voltages in the CLIQ circuit.

1. Introduction

Superconducting (SC) wires are needed for the windings of magnetic resonance imaging (MRI) magnets. These wires are used as parts of background (static) field coils which provide stable and strong magnetic fields. Niobium-titanium (NbTi) wires are widely used in MRI, but magnesium diboride (MgB₂) is a promising material due to its higher critical temperature (T_c) compared to NbTi, adequate engineering current density, simplicity in fabrication, and affordability [1]. A number of groups explored MgB₂ SC wires' use in the windings of MRI background field coils [2,3], but quench protection requires attention, because MgB₂ has higher T_c and therefore a slower normal zone propagation.

1.1 Quench and its mitigation

In this paper, quench protection of MgB₂ segmented coils is discussed. A quench is a sudden and irreversible change from a SC state to a normal state, resulting in the melting or degradation of the wire



due to joule heating. The purpose of any quench protection system (including CLIQ system) is to prevent the burn-out of a wire segment due to a localized hot zone [4]. A quench is initiated by a small perturbation [5], which can stem from, for example, vibration and epoxy cracking. When epoxy cracks, this small mechanical perturbation, via friction, may lead to a slight increase in the temperature of a short length of the SC wire. This may initiate an instability cycle until T_c is exceeded, and a localized normal zone created. Because the normal zone is small, the heat may be sufficient to damage the coil. To mitigate this problem, quench protection is applied in which the heat begins to spread along a large section of the wire. This allows for quench recovery, and as the whole SC wire tends to the normal state, the circuit resistance increases, and transport current decreases to some safe level.

There are two ways to heat up the entire coil: from inside the winding by AC loss (or other mechanism) or from outside by external heaters. The generation of heat by AC loss can be achieved by the CLIQ circuit which delivers an AC current to the SC coil when a quench is detected [5]. The AC loss has several types: hysteresis loss, eddy current loss, coupling loss, and transport current loss. The CLIQ system was developed applicable to the beam guidance magnets of high energy particle accelerators at CERN [4,6]. Poole et al. [3,7] applied CLIQ to MRI coils, but this is problematic because MRI coils have higher inductances. A change in Poole's coil design (one coil inside another) resulted in lower inductances and low required initial voltages. According to our previous work, the voltage required for a single MRI coil was high, leading to the need of multiple CLIQ sets. To address the coil fabrication difficulty, Poole's split coil designs can be modified from a design with one coil inside another to one where two coils side by side. These two coils are configured in series such that during normal operation their DC magnetic field added. If a quench is detected, the CLIQ circuit injects AC at a tap between these two coils, and this drives AC magnetic fields in both that tend to cancel each other. This reduces the effective inductance significantly. The mutual inductance and effective inductance were calculated to be ~ 0.01 H [8]. Coming back to the fact that the required voltage is too high, we need to modify this approach.

In this paper, we have explored doing this via simultaneous overcurrent using Joule heating in the matrix. As a part of this effort, the total AC and ohmic loss generated was calculated in Open Modelica. We explored if the coil could be protected by driving it fully normal with either (a) an applied over-current, (b) an induced AC current, or (c) some combination of both.

1.2 Lumped parameter model for superconducting systems

Finite element models (FEMs) are widely used for investigating the magnetic flux density, AC loss, and critical current of superconductors [9,10,11], but FEM is highly time-consuming. Unlike FEMs, lumped parameter models (LPMs) produce faster simulations by representing the system to be modelled as a network of lumped components, each with their own resistance, inductance, capacitance, thermal conductance, and heat capacity [12]. In past work, LPMs of high temperature SC components were validated by comparing the results with those obtained by FEM [13,14,15]. This work is the result of a detailed investigation of the LPM modelling a SC composite, and a modified CLIQ system with it. The SC composite model in Open Modelica included both thermal and electrical components, and described the interface between the SC coil and its environment. It included the fact that the superconductor behaviour depends on temperature, magnetic field, and current. In this case, the SC coil was simulated to be in our liquid-helium free cryostat [2]. Subsequently, the composite model was inserted back into the CLIQ circuit and its behaviour in an operating circuit was explored.

2. Simulation

2.1 Superconducting composite model

A SC composite model was developed in Open Modelica using a lumped parameter model. We used Open Modelica to define a segment of a SC composite (MgB_2/Cu) and its dependence on current and temperature. Critical current density depends on the temperature, according to [16],

$$J_c = J_{c0} \left(1 - \tanh\left(\frac{T}{T_c}\right) \right) \quad (1)$$

where J_{c0} is the critical current density at zero temperature and T is the operating temperature. It follows that I_c decreases as the temperature increases. We used the hyperbolic tangent (T/T_c) rather than (T/T_c) to avoid numerical instability.

Table 1. Superconducting composite specifications

Parameters	Value (unit)
Critical electrical field (E_c)	1e-4 (V/m)
Critical current of SC filament (I_c)	150 (A)
Resistivity transition index (N)	13
Length of wire (L)	1 (km)
Superconducting fraction of wire segment (λ)	0.5
Critical temperature (T_c)	40 (K)
Wire diameter (D)	1 (mm)
Twisted pitch (Lp)	5 (mm)

representing the contribution from impurities and other defects [19]. Table 1 lists the specifications of our SC composite.

2.2 Mathematical methods

The hysteresis loss can be described by the following expression,

$$P_c = \frac{8}{3\pi} B f \lambda J_c d_s \quad (2)$$

where P_c is AC power loss per unit volume (W/m^3), f is the frequency of the applied magnetic field, λ is area fraction of superconducting filaments, d_s is the diameter of the strand, and B is the applied AC magnetic field [20]. Coupling loss makes a large contribution to heat generation and stability of twisted MgB_2 cables at high frequencies. Coupling loss, generated in the matrix material, is given by [21]:

$$P_c \left[\frac{\text{W}}{\text{m}^3} \right] = \frac{1}{n \rho_{eff}} (f L_p B)^2 \quad (3)$$

where n is the geometric factor, (equal to 2 for a round multifilamentary wire) L_p is the twist pitch, ρ_{eff} , the effective resistivity, is given by $\rho \frac{1-\lambda}{1+\lambda}$ for low filament matrix interface resistance [22]. In addition, heating by ohmic loss is generated when overcurrent flows into the matrix when the temperature of the composite is above T_c , i.e. when the superconducting filaments reach the normal state.

2.3 Circuit design

Figure 1 (right) is our SC composite model and displays both the thermal and electrical components in four blocks. The central block represents our SC wire segment composed of the monofilament wire and its stabilizer. The “fixed temp” block represents the temperature of the environment (4.2 K). The “thermal conductance (G)” block represents the interface between SC composite and its environment. The value of G is the operating power of the cryocooler (approximately 30 W at 15 K). The “heat capacity (C)” means the heat capacity of the SC wire itself (the amount of stored heat). The value of C (estimated to be 480 J/K) is given by $c_p m / \Delta T$, where c_p is the specific heat capacity of MgB_2 , m is the total mass of the SC core filament.

3. Result and Discussion

In our initial work, we performed circuit simulations to examine the possibility of applying CLIQ quench protection to a MgB_2 MRI magnet segment [2]. The simulations calculated the charging voltages and capacitances associated with various excitation currents and numbers of split coils. The largest challenge was controlling the maximum circuit voltages. A high voltage across the coil might burn it out.

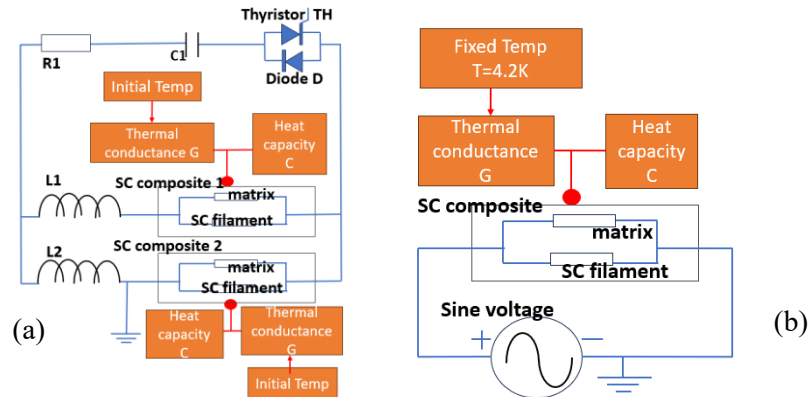


Figure 1: (a) shows the electrical diagram of our modified CLIQ system. (b) Our model of a SC composite (MgB_2/Cu) conduction cooled and driven by an AC power supply. Two SC composite models were put beside L1 and L2 in the full circuit, for total system simulation

As noted above, one way to avert this is to subdivide the coil. Given that the AC loss power and energy were being maintained, the coil could be subdivided into two equal segments. The excitation of these two half-coils, such that they had opposing magnetic fields during quench protection AC loading, suppressed the effective inductance down to the levels of 0.01 H. It follows that the split coil design leads to a reduced circuit voltage. However, this reduction is still not sufficient. Modifying the CLIQ approach by adding in an overcurrent excitation ($I > I_c$) will allow further voltage reductions while still generating sufficient protection heating of the magnet segment. We built a lumped parameter model in Open Modelica to describe the electrical and thermal behaviour of the magnet segment when $I > I_c$.

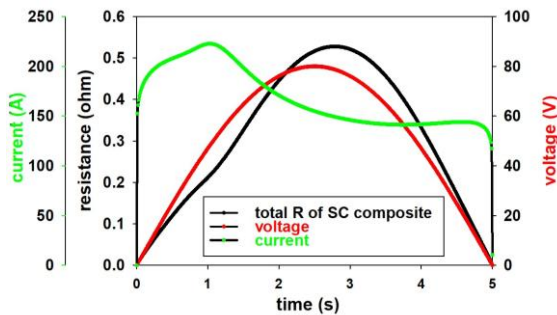


Figure 2: Total resistance, current, voltage of superconducting composite (MgB_2/Cu) as a function of time at 0.1 Hz with 80 V AC power applied, for the first cycle. Temperature starts at 4.2 K.

T vs time increases during 0~1s, while it decreases during 1~3 s. T vs time drops back to 6 K from 3~5 s. The current vs time increases during 0~1 s, and it decreases and flattens out during 1~5 s. Superconductors currents share when their temperature is between the current sharing temperature (T_{cs}) and T_c ($T_{cs} < T < T_c$) [5]. The current after 5 s is smaller than that after 1 s, due to the smaller I_c caused by temperature increase.

The frequency was increased from 0.1 Hz to 1 Hz and 10 Hz to generate more coupling loss and to increase the temperature. The voltage supply also provided various excitation voltages from 10 V to 80 V. The maximum current, the time of T to reach T_c and the resistance of the composite model was modelled.

This SC composite was initially modelled with 80 V, 0.1 Hz AC power applied. This model achieved the SC and normal states during the first charging cycle. In **Figure 2**, the starting temperature (time=0 s) is 4.2 K. The current (I) is 0 A at 0 s, because the quench protection circuit is not initiated. When the sinusoidal voltage starts, the current that runs through the SC filaments is mostly equal to I_c (150 A). The sinusoidal voltage then increases during 0~2.5 s, the maximum voltage (V_{max}), which is obtained after 2.5 s, decreases to 0 after 5 s. The temperature (T) increases from 4 K to a maximum value of 10 K during 0~3 s when the resistance (R) slope during 0~1 s is smaller than that during 1~2.5 s. This is because the slope of

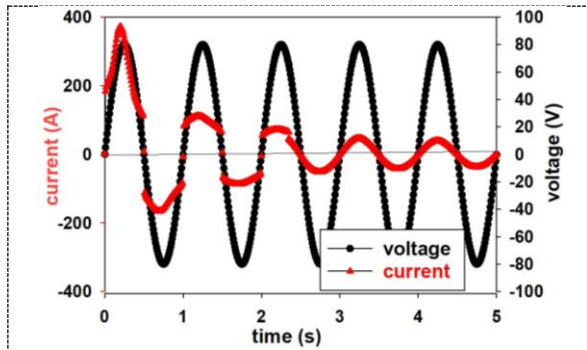


Figure 3. The Curves of current and voltage of the SC composite (MgB_2/Cu) at 1Hz as a function of time after applying a voltage of 80V.

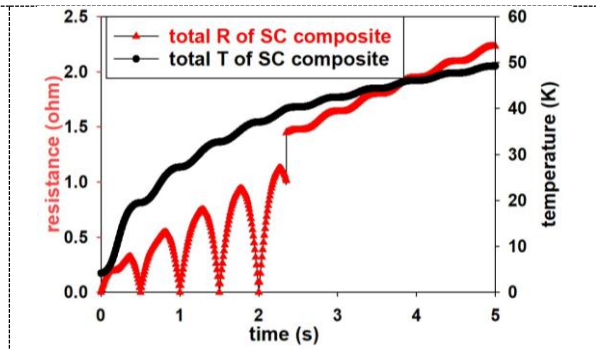


Figure 4. The Curves of total resistance and temperature of the SC composite (MgB_2/Cu) at 1Hz ($T_c=40\text{K}$) as a function of time after applying a voltage of 80V.

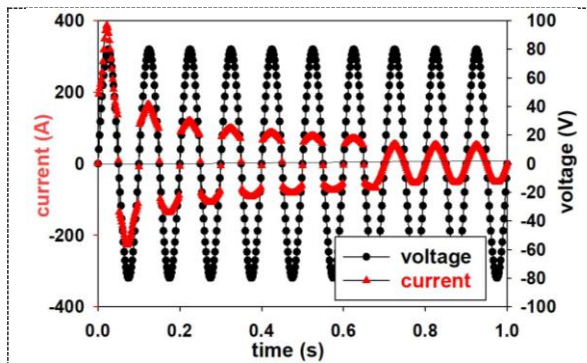


Figure 5. The Curves of current and voltage of the SC composite (MgB_2/Cu) at 10Hz as a function of time after applying a voltage of 80V.

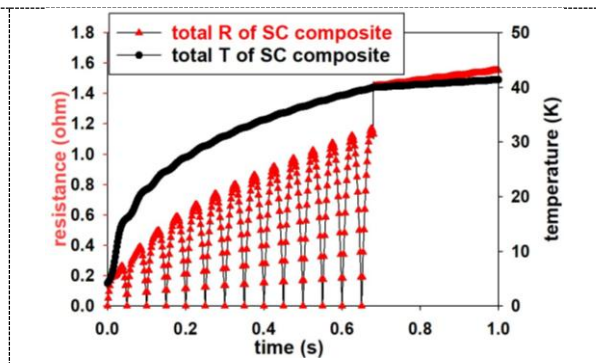


Figure 6. The Curves of total resistance and temperature of the SC composite (MgB_2/Cu) at 10Hz ($T_c=40\text{K}$) as a function of time after applying a voltage of 80V.

Table. 2. Effect of excitation voltage on SC composite properties at 0.1 Hz, external magnetic field 3 T, critical temperature 40 K, and critical current 150 A.

Excitation voltage (V)	Max current (A)	Time of T to reach T_c (s)	SC max R at T_c (ohm)	Total max R at T_c (ohm)	Power generated by overcurrent (kW)	Power generated by coupling current (W)
10	14	29	E-13	E-13	0.14	2.94
20	200	13	0.4	0.3	4.0	2.94
40	240	6.1	0.9	0.6	9.6	2.94
80	390	2.5	5	1.1	31.2	2.94

Increasing the excitation voltage increases the ohmic loss in the matrix and decreases the time for the coil temperature to exceed T_c . The total resistance (**Figures 4 and 6**) is equal to the SC resistance in parallel with the matrix resistance. The SC returns to the normal state when $T > T_c$. At 10 Hz, coupling loss dominates the heating, while at 0.1 Hz ohmic loss dominates. In a previous work, we simulated that it took 8 seconds for the coil to heat up and burnt out. It follows that this size of MRI coil is protectable. Overcurrent technique can be seen to generate enough heat compared to coupling loss at high frequencies and ohmic loss at low frequencies.

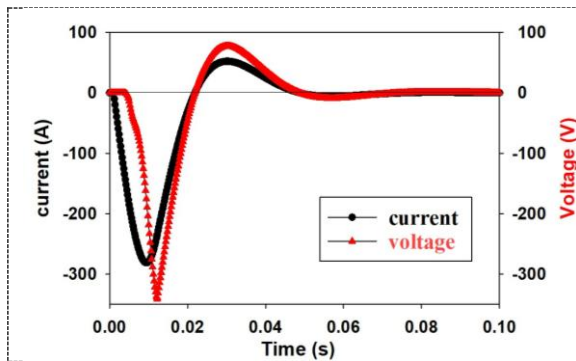
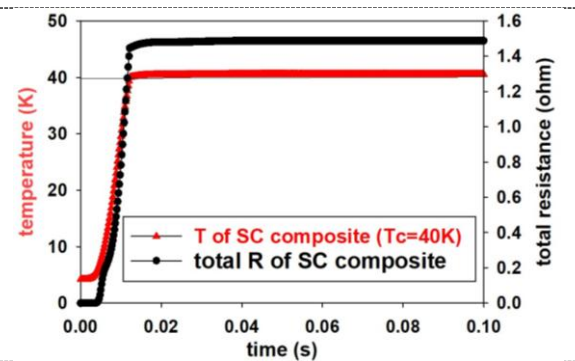
Table. 3. Effect of excitation voltage on SC composite properties at 1 Hz, external magnetic field 3 T, critical temperature 40 K, and critical current 150 A.

Excitation voltage (V)	Max current (A)	Time of T to reach T_c (s)	SC max R at T_c (ohm)	Total max R at T_c (ohm)	Power generated by overcurrent (kW)	Power generated by coupling current (kW)
10	190	19	0.2	0.2	1.9	0.29
20	205	11	0.3	0.3	4.1	0.29
40	230	5.4	0.6	0.6	9.2	0.29
80	370	2.3	5	1.1	29.6	0.29

Table. 4. Effect of excitation voltage on SC composite properties at 10 Hz, external magnetic field 3 T, critical temperature 40 K, and critical current 150 A.

Excitation voltage (V)	Max current (A)	Time of T to reach T_c (s)	SC max R at T_c (ohm)	Total max R at T_c (ohm)	Power generated by overcurrent (kW)	Power generated by coupling current (kW)
10	185	0.57	0.2	0.2	1.8	29.4
20	203	0.55	0.3	0.3	4.1	29.4
40	236	0.52	1.1	0.6	9.4	29.4
80	410	0.45	5	1.1	32.8	29.4

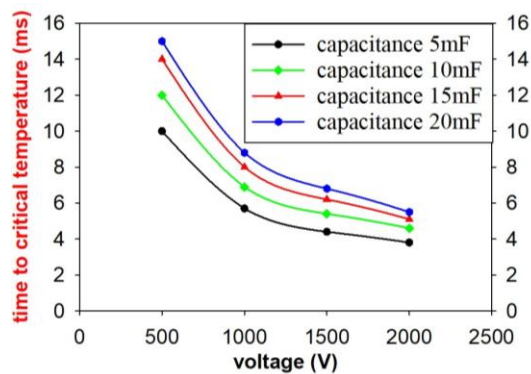
After the SC module was returned to the CLIQ circuit. The currents and voltages of the SC composite were simulated at different capacitor sizes and charging voltages. The SC module was connected with a 10 mF capacitor charged 500 V in the CLIQ circuit (see **Figure 1**, left). When the quench is detected, an AC current is delivered from the capacitor forming a LC resonance circuit. In **Figure 7**, the current and voltage are excited and decayed within 0.07 s. In **Figure 8**, the temperature of the SC composite is raised by the heat of coupling and ohmic losses to T_c within 0.02 s. The quench protection is completed when the whole SC composite is heated up to the normal state. Capacitor sizes and charging voltages are varying from 5 to 20 mF and from 0.5 to 2 kV respectively to investigate the coupling and ohmic loss effect on heating the SC composite.

**Figure 7.** The Curves of current and voltage of the SC composite (MgB_2/Cu) at 50Hz as a function of time using a 10mF capacitor charged 500V in the CLIQ circuit.**Figure 8.** The Curves of total resistance and temperature of the SC composite (MgB_2/Cu) at 50Hz as a function of time using a 10mF capacitor charged 500V in the CLIQ circuit.

Coupling and ohmic losses of the SC composite in the modified CLIQ system were calculated and listed (see **Table 5**). In CLIQ circuit, the frequency of the coupling loss generated in SC composite depends on the capacitor size and the total inductance of coils. High capacitance leads to a low frequency coil. Ohmic loss depends mainly on the charged voltage of the capacitor.

Table 5. Effect of excitation voltage on SC composite properties at 10Hz, external magnetic field 3 T, critical temperature

Capacitance (mF)	5 (71 Hz)	10 (50 Hz)	15 (41 Hz)	20 (36 Hz)
AC loss	1.47 MW	0.73 MW	0.49 MW	0.37 MW
Ohmic loss (500 V)	0.22 MW	0.28 MW	0.32 MW	0.35 MW
Ohmic loss (1 kV)	0.35 MW	0.88 MW	0.99 MW	1.08 MW
Ohmic loss (1.5 kV)	1.43 MW	1.74 MW	1.92 MW	2.05 MW
Ohmic loss (2 kV)	2.44 MW	2.88 MW	3.14 MW	3.32 MW

**Figure 9:** The curves of time of temperature of SC composite (MgB₂/Cu) to reach T_c as a function of charged voltage of the capacitor in the CLIQ circuit.

CLIQ circuit. The temperature of the SC composite coil could be raised quickly (within 1 s) to the critical temperature by coupling loss and ohmic loss. This mixed approach using split coils and overcurrent in the matrix material can protect MRI SC background coils efficiently and quickly.

The properties of the SC composite in the modified CLIQ circuit are consistent with the result of a previous simulation that of a SC composite with an AC voltage supply in **Table 2,3,4**. Coupling loss contributes more heat at high frequencies and ohmic loss provides more heat at low frequencies given at viable voltages across the charged capacitor in the CLIQ circuit.

4. Conclusions

The split coil design and the overcurrent technique were shown to generate enough heat to protect the coil against quench. A split coil design was shown to decrease the inductance of MRI SC coils to 0.01 H. Our SC module performed well when connected to an AC voltage supply and a modified

Acknowledgments

This work was supported by the National Institute of Biomedical Imaging and Bioengineering, under grant R01EB018363.

References

- [1] Vinod K, Abhilash Kumar R G, and Syamaprasad U 2006 Prospects for MgB₂ Superconductors for Magnet Application *Supercond. Sci. Technol.* **20** R1 (doi:10.1088/0953-2048/20/1/R01)
- [2] Zhang D, *et al* 2018 Instrumentation, Cooling, and Initial Testing of a Large, Conduction-cooled, React-and-wind MgB₂ Coil Segment for MRI Applications *Supercond. Sci. Technol.* **31** 085013 (doi:10.1088/1361-6668/aacae3)
- [3] Poole C, Baig T, Martens M, and Al Amin A 2019 Mechanical Analysis of an MgB₂ 1.5 T MRI Main Magnet Protected Using Coupling Loss Induced Quench *Cryogenics* **100** 18–27 (doi:10.1016/j.cryogenics.2019.02.005)
- [4] Ravaioli E, Datskov V I, Giloux C, Kirby G, ten Kate H H J, and Verweij A P 2014 New, Coupling Loss Induced, Quench Protection System for Superconducting Accelerator Magnets *IEEE Transactions on Applied Superconductivity* **24** 0500905 (doi:10.1109/TASC.2013.2281223)
- [5] Bottura L 2014 Cable Stability arXiv:1412.5373
- [6] Ravaioli E *et al* 2016 First Implementation of the CLIQ Quench Protection System on a 14-M-Long Full-Scale LHC Dipole Magnet *IEEE Transactions on Applied Superconductivity* **26** 4000505 (doi:10.1109/TASC.2015.2510400)

- [7] Poole C, Baig T, Deissler R J, and Martens M 2017 Numerical Analysis of the Coupling Loss Induced Quench Protection for a 1.5 T Whole-Body MgB_2 MRI Magnet *Supercond. Sci. Technol.* **30** 105005 (doi:10.1088/1361-6668/aa824c)
- [8] Purcell E M and Morin D J 2013 Electricity and Magnetism *Cambridge University Press* p 359-367
- [9] Liang F *et al* 2017 A Finite Element Model for Simulating Second Generation High Temperature Superconducting Coils/Stacks with Large Number of Turns *J. Appl. Phys.* **122** 043903 (doi:10.1063/1.4995802)
- [10] Grilli F *et al* 2005 Finite-Element Method Modeling of Superconductors: From 2-D to 3-D *IEEE Transactions on Applied Superconductivity* **15** 17-25 (doi:10.1109/TASC.2004.839774)
- [11] Amemiya N, Murasawa S, Banno N, and Miyamoto K 1998 Numerical Modelings of Superconducting Wires for AC Loss Calculations *Physica C: Superconductivity* **310** 16-29 (doi:10.1016/S0921-4534(98)00427-4)
- [12] dos Santos G, Martins F G R, Sass F, Dias D H N, Sotelo G G and Morandi A 2021 A Coupling Method of the Superconducting Devices Modeled by Finite Element Method with the Lumped Parameters Electrical Circuit *Superconductor Science and Technology* **34** 045014 (doi:10.1088/1361-6668/abe600)
- [13] Baez-Munoz A, Trillaud F, Rodriguez-Rodriguez J R, Castro L M, and Escarela-Perez R 2021 Thermoelectromagnetic Lumped-Parameter Model of High Temperature Superconductor Generators for Transient Stability Analysis *IEEE Transactions on Applied Superconductivity* **31** 1-5 (doi:10.1109/TASC.2021.3060696)
- [14] Hearn C S, Pratap S B, Chen D, and Longoria R G 2014 Lumped-Parameter Model to Describe Dynamic Translational Interaction for High-Temperature Superconducting Bearings *IEEE Transactions on Applied Superconductivity* **24** 46-53 (doi:10.1109/TASC.2014.2298112)
- [15] Ravaioli E, Auchmann B, Maciejewski M, ten Kate H H J, and Verweij A P 2016 Lumped-Element Dynamic Electro-Thermal Model of a Superconducting Magnet *Cryogenics* **80** 346-356 (doi:10.1016/j.cryogenics.2016.04.004)
- [16] Goodrich L F and Bray S L 1990 High Tc Superconductors and Critical Current Measurement *Cryogenics* **30** 667-677 1990 (doi:10.1016/0011-2275(90)90229-6)
- [17] Koch C C and Easton D S 1977 A review of mechanical behaviour and stress effects in hard superconductors *Cryogenics* **17** 391-413 (doi:10.1016/0011-2275(77)90288-0)
- [18] Gilev S D 2019 Electrical Resistance of Copper at High Pressures and Temperatures: Equilibrium Model and Generation of Defects of the Crystal Structure under Shock Compression *Combustion, Explosion, and Shock Waves* **55** 620-628 (doi:10.1134/S0010508219050149)
- [19] Fickett F 1983 Electrical Properties. In: Materials at Low Temperatures *American Society for Metals* p 195
- [20] Oomen M P 2000 AC loss in superconducting tapes and cables *University of Twente*
- [21] Collings E W, Sumption M D, Susner M A, Dietderich D R, and Nijhuis A 2011 Coupling Loss, Interstrand Contact Resistance, and Magnetization of Nb_3Sn Rutherford Cables with Cores of MgO Tape and S-Glass Ribbon *IEEE Transactions on Applied Superconductivity* **21** 2367-2371 (doi:10.1109/TASC.2010.2083620)
- [22] Carr Jr W J 2001 AC Loss and Macroscopic Theory of Superconductors *CRC press* p 127,188